Reliable and easy-to-use SERS spectroscopy probe using a tapered opto-fluidic photonic crystal fiber

Amine Benazza, Flavien Beffara, Jean-Louis Auguste, Malini Olivo, U S Dinish, Georges Humbert

Research Article Vol. 32, No. 3 / 29 Jan 2024 / Optics Express 3440
Optics EXPRESS

Reliable and easy-to-use SERS spectroscopy probe using a tapered opto-fluidic photonic crystal fiber

AMINE BENAZZA,[1] FLAVIEN BEFFARA,[1] JEAN-LOUIS AUGUSTE,[2] MALINI OLIVO,[1,3] U. S. DINISH,[2,4] AND GEORGES HUMBERT[1,5]

[1]XLIM Research Institute, UMR 7252 CNRS / Limoges University, 123 av. A. Thomas, Limoges 87000, France
[2]A*STAR Skin Research Labs (A*SRL), Agency for Science, Technology and Research (A*STAR), 31 Biopolis Way, #07-01 Nanos, Singapore 138669, Singapore
[3]Malini_Olivo@asrl.a-star.edu.sg
[4]Dinish@asrl.a-star.edu.sg
[5]georges.humbert@xlim.fr

Abstract: Surface enhanced Raman spectroscopy (SERS) is one of the most sensitive biosensing techniques that offers label free detection for a variety of applications. Generally, SERS spectroscopy is performed on nano-functionalized planar substrates with plasmonic structures or colloidal nanoparticles. Recently, photonic crystal fibers (PCFs) have gained great interest for SERS based bio sensing applications due to the immense advantages such as improved sensitivity, flexibility and remote sensing capability that it offers compared to the planar substrates. However, the use of PCF based biosensors demand the alignment of it under a microscope, which can affect the reliability of SERS measurements and could be restrictive for practical end use applications. Herein, we aim to develop a tapered suspended core PCF fiber (Tapered-SuC-PCF) that represents an improvement in coupling efficiency and measurement reliability as well as it opens the way to the development of an easy-to-use bio-sensing probes with a plug and play option with conventional Raman spectrometers. We have fabricated several samples of the optimized tapered-SuC-PCF and demonstrated its superior SERS performance compared to standard SuC-PCF fibers with 2 μm core diameter. An excellent SERS measurement reliability is demonstrated using such a fiber in a plug and play type system demonstrating its versatility for practical end use applications.

1. Introduction

Surface-enhanced Raman spectroscopy (SERS) is one of the most interesting noninvasive detection techniques due to the high specificity of Raman vibration modes and the sensitivity offered by plasmonic enhancement [1]. It allows simultaneous detection [2–6] of multiple analytes in relatively small volumes with minimal sample preparation [7]. Since the Raman cross-section of molecules is very weak, SERS enables Raman signal enhancement in the order of at least 10^6, through the amplification of electromagnetic fields generated by the excitation of localized surface plasmon resonances (LSPR) [8–14] in specially designed nanostructured materials. This result in the giant enhancement of fingerprint Raman spectra of molecules, which are located in the close proximity (~ 10-20 nm) to the nanostructured surface [15–18]. Generally, SERS spectroscopy is performed on nano-functionalized planar substrates with plasmonic structures. Excitation light/analyte interactions and collection of the SERS signal occur over a very limited area (a few micrometers in diameter), which corresponds to the focal point of the laser. Moreover, the sensitivity, reproducibility and repeatability of SERS measurements are very sensitive to parasitic irregularities of plasmonic nanostructures, which limits the reliability

#501911 https://doi.org/10.1364/OE.501911
Journal © 2024 Received 28 Jul 2023; revised 13 Dec 2023; accepted 17 Dec 2023; published 18 Jan 2024

Optics EXPRESS

of quantitative analyses. photonic crystal fibers (PCFs) composed of microfluidic channels adjacent to the cores, have gained interest for SERS spectroscopy of extremely small volumes of fluids [19]. These PCFs promote SERS interactions over a very long length, which significantly enhances the Raman signal. Contrary to planar substrates that allow only two dimensional of interaction, these PCFs lead to a three dimensions of interaction along the entire fiber length, which allows an improvement in sensitivity [20–25]. Moreover, the nano-functionalization of the fibers with plasmonic nanoparticles (ex. gold nanoparticles) and the optimization of the size of the core to match with the microscope of the Raman spectrometer allowed us to obtain an excellent reliability of the measurements [26]. Furthermore, since the light interact with NPs over significantly larger area, minute irregularity in the deposition of NPs do not affect the reliability in measurements, contrary to planar substrates. In this work, special designs of PCF fibers lead to do such an application as SuC-PCF fibers, which are characterized by a silica sheath composed of three air holes arranged around a core. Sensing with SuC-PCF is established on using Raman spectroscopy and evanescent wave field (EF) interaction [19]. The presence of the solid core inside the fiber lead to guide the light due to total internal reflection (TIR), while the air holes can be used as channels to circulate micro-fluids along the entire length of the fiber and thus promote an interaction between the micro-fluids and the partial overlap of the guided evanescent electromagnetic wave. The performance of PCFs-based sensor relies on the core size, a bigger core size improve the light coupling efficiency with Raman spectrometer and the reliability of SERS measurements. In other hand, a smaller core size is required to have a high fraction of EF that interact with NPs and analyte, which allow an improvement in sensitivity [27]. However, the current configuration requires alignment under a microscope, posing limitations leading to increased effect of misalignments on the measurement reliability. This demands significant time and expertise to realize the precise alignment and efficient measurements. Consequently, there is a serious need to look for an alternative approach that relieve the dependence on microscope-based alignment, offering a more easy-to-use and strong solution for accurate measurements in practical environment.

This work presents a novel approach of SERS sensing through the development of an original fiber-based SERS sensing platform using a tapered SuC-PCFs enabling efficient, simple and easy-to-use with a plug and play type system. It is realized by optimizing the fiber core diameter to ensure excellent coupling efficiency. Subsequently, a tapered fiber was fabricated from this initial fiber by reducing the core diameter along length in order to achieve optimal sensitivity and signal enhancement. This tapered fiber is tested by incorporating it into the plug and play system for measurement process without the need for realignment each time. This approach, combing optimized fiber fabrication, tapering process and the user-friendly plug and play system, resulted in a highly sensitive and reliable SERS platform that has potential translation for practical end use application. Herein, we perform a numerical investigation of the design parameter of the tapered-SuC-PCF, and its impact on the coupling efficiency of the fiber with Raman spectrometer. Then, fabrication and characterization of optimized tapers were realized. The SERS performance of these tapers was subsequently tested, particularly in terms of the reliability of SERS measurements. Finally, the employment of the taper within a plug and play optical system was evaluated.

2. Numerical simulation

In order to evaluate the coupling efficiency between the SuC-PCF and the Raman spectrometer, we have calculated, with the finite element method, the overlap integral of the electromagnetic field distributions of the fundamental mode of SuC-PCF with the Gaussian beam of the excitation laser [28,29]. The diameter of the Gaussian beam corresponds of the measured focused laser beam on our experimental setup. Its diameter at half maximum is approximately 2 μm, the emission wavelength is 785 nm and the laser is linearly polarized. From these parameters, we

Optics EXPRESS

have generate 2D matrix of each components of the electromagnetic field distribution of the incident beam (with a linear polarization).

To simulate possible misalignment during the measurements, the center of the incident beam was randomly positioned on 200 points within a 1 µm radius disk (Fig. 1(b)) which could represent the laser coupling positioning error on the fiber core.

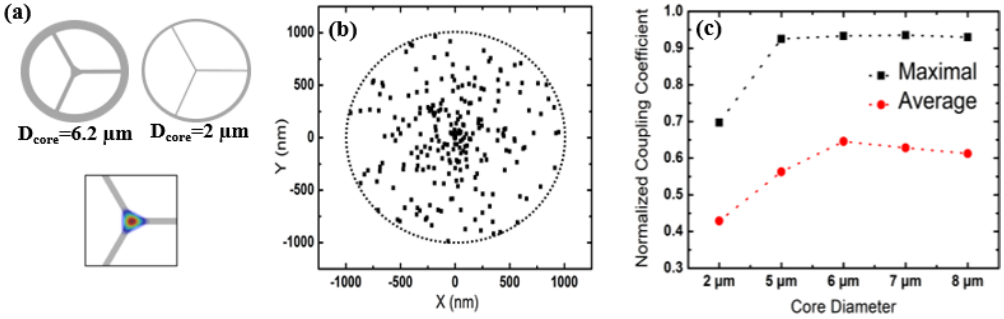

Fig. 1. (a) Design of SuC-PCFs used in the simulation with different core sizes. (b) Distribution of the center of the laser beam randomly positioned (200 times) within an area limited by a circle of 1 µm radius around the center of the fiber. (c) Maximal and average coupling coefficient values for SuC-PCFs with different core diameters.

Once the electromagnetic field distributions of the incident beam and of the fundamental mode were calculated, the normalized coupling coefficient (C) was deduced from the continuity of the transverse field components over the cross-section of the fiber, between the incident beam and a fiber mode, following this equation [29]:

$$C = \frac{1}{4} \times \frac{\int (\vec{E}^*_{in}(x,y) \times \vec{H}(x,y) + \vec{E}(x,y) \times \vec{H}^*_{in}(x,y)) dxdy}{\sqrt{\frac{1}{2}\int Re(\vec{E}_{in}(x,y) \times \vec{H}^*_{in}(x,y)) dxdy} \times \sqrt{\frac{1}{2}\int Re(\vec{E}(x,y) \times \vec{H}^*(x,y)) dxdy}}$$

With $E_{x/y}$ and $H_{x/y}$ are the x and y components of the electric and magnetic fields of the fundamental mode guided inside the fiber. $E_{x/y\ in}$ and $H_{x/y\ in}$ are the x and y components of the electric and magnetic fields of the laser Gaussian beam.

Figure 1(c) represents the normalized coupling coefficient between the incident Gaussian beam and the fundamental mode of SuC-PCFs with different core diameters. As expected, when the laser beam is in the center of the core, the highest coupling efficiency is obtained. The SuC-PCF with a core diameter of 6 µm exhibits the highest average normalized coupling coefficient (0.64) with a normalized maximal coupling coefficient (0.93) similar to other SuC-PCF. This SuC-PCF design (Dcore = 6 µm) was then selected, fabricated, and used in the experimental studies.

3. Fabrication of fibers

3.1. SuC-PCFs

SuC-PCFs were fabricated through the stack-and-draw process [30], by stacking three capillaries (drawn from a silica tube) into a silica tube. The preform is drawn down to cane (of few millimeter) that is inserted into a jacket tube and finally drawn to fibers. The cladding thickness and core size are controlled by adjusting pressure, preform descent speed and drawing speed. The fabrication of large holes were also controlled for enabling easily analyte infiltrations. Scanning electron microscope (SEM) was used to precisely determine the dimensions of the fibers. Figure 2(a) and (c) show SEM images of two fibers with a core diameter of 2 µm and 6.2 µm respectively. These fibers are named: 2 µm-PCF and 6.2 µm-PCF, respectively, in the following. Figure 2(b) shows

Optics EXPRESS

the zoom-in SEM picture of core of the 2 µm-PCF. The three struts showed in these figures form the core of the fiber that guide the light based on the TIR principle. A portion of the evanescent light in the holes will interact with the analyte injected inside the fiber. The 6.2 µm-PCF was used subsequently to fabricate a tapered-SuC-PCF with local reduction in fiber diameter.

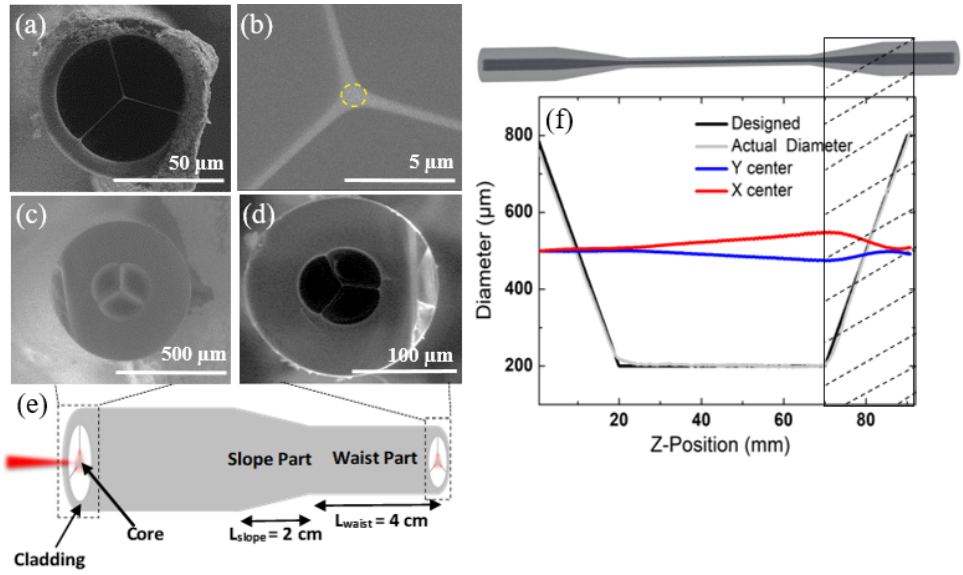

Fig. 2. SEM picture of the cross section of: (a) 2 µm-PCF. (b) Zoomed image of 2 µm-PCF. (c) Input of the tapered-PCF. (d) SEM picture of the cross section in the waist part of the tapered-PCF. (e) Schematic of the tapered-PCF. (f) Variation of outer diameter with Z-position (gray curve) and variation of the center of the fiber relative to the screen (X center, red curve) and (Y center, blue curve).

3.2. *Tapered-SuC-PCFs*

To fabricate the tapered-PCF from the original 6.2 µm-PCF, a Fujikura LZM 100 fusion splicer is used. This system allows precise control over positions calibration along the X-axes and Y-axes and incorporates motors that enable the movement of the fiber and the application of CO_2 laser. This specialized splicing system uses a CO_2 laser instead of filaments or electrodes, which offers the elimination of any deposits on the fiber surface. The tapers are fabricated by heating and stretching locally the fiber during its translation (in front of the laser beam) with a speed difference between two motors (i.e., the pulling motor is faster than the feeding motor). Simultaneously, the CO_2 laser is focused on a predefined zone of the fiber.

Figure 2(d) shows a SEM picture of the cross section at the waist of the tapered-PCF illustrating a homothetic reduction of the fiber without geometrical deterioration. The dimensions of the manufactured samples are plotted in Fig. 2(e): an initial fiber portion (D_{ext} = 815 µm, D_{core} = 6.2 µm) of 2 cm long length, then a transition section of 2 cm with gradual reduction, and a 4 cm long length tapered waist with D_{ext} = 200 µm and D_{core} = 1.7 µm. To maintain the internal structure of the fiber while reducing its diameter, we adjusted various parameters, including laser power, pulling speed, and feeding speed. This resulted in a successful reduction of the core diameter in the waist section to below 2 µm. The laser power was about 16.07 W in the taper transitions and 14.4 W in the waist. The speed of the feeding motor was set at 0.06 mm/s. The speed of the pulling motor was adjusted with the control-software for matching the targeted taper profile.

Optics EXPRESS

As shown on Fig. 2(f), the evolution of the external diameter of the tapered fiber (gray curve) matches with the expected one (black curve). However, there was a minor distortion in the tapered structure, causing misalignment with the central axis (i.e., slight shift between X-center and Y-center on Fig. 2(f)), that is formed at the end of the fabrication process. This part of the taper was removed without consequence on the measurements as our experimental setup was designed to collect the backscattered Raman signal.

4. Results and discussion

4.1. Experimental setup used and coupling efficiency measurements

Figure 3 shows the setup used for SERS experiments. We used a wavelength-stabilized laser diode (Thorlabs LP785-SAV50) emitting up to 50 mW at the wavelength of 785 nm. The laser diode was pigtailed with single mode fiber. At the fiber output, the laser beam passes through the collimation lens and a cleaning band-pass filter, and then it is reflected by the dichroic mirror, coupled into the sample using a 40x objective lens. It is important to note that SERS measurements for all fibers were consistently obtained using the same 40x objective lens and a laser power of 9.9 mW. The backscattered Raman signal passes through the same objective lens, a long-pass filter, and is collected by a multimode fiber leading to the Raman spectrometer (QE PRO – Ocean Insight). The integration time is fixed at 10 s, and no signal averaging is applied. For calibration, we utilize the robust silica Raman signal at 520 cm^{-1} as a reference, ensuring that we achieved the same intensity consistently before the initiation of each measurement. Baseline correction was systematically applied to the spectra to remove the background and fluorescence bands. We utilize a specialized software (MainRaman) with adjustable parameters to fine-tune the baseline correction settings, ensuring a precise determination of the level of background removal for all spectra. Importantly, this consistent background subtraction across all spectra enables us to quantify the intensity of each peak with precision. A CDD camera was used to visualize the input side of the fiber for the alignment and to ensure that the laser beam is focused on the same location of the core fiber for each measurement.

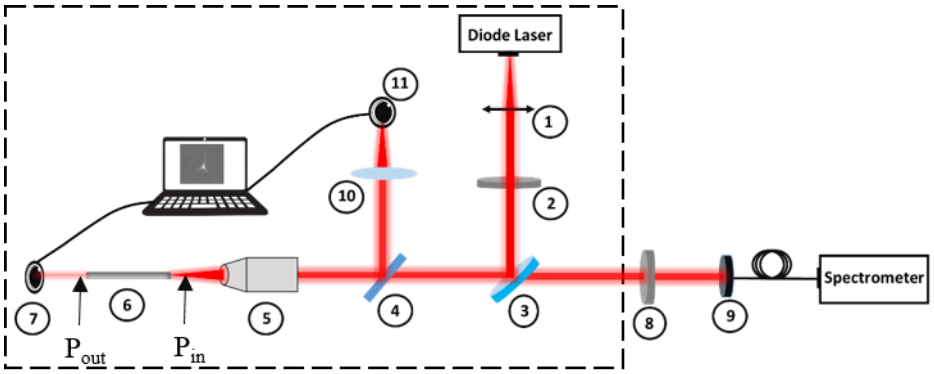

Fig. 3. Experimental setup used for SERS measurements with our SuC-PCF probes. 1: Collimator; 2: Band-pass filter; 3: Dichroic Mirror; 4: Beam Splitter; 5: 40x Microscope objective lens; 6.2: SuC-PCF under measurements positioned on a XYZ translation stage; 7: Camera of output; 8: Long pass filter; 9: Raman signal collector (collector lens with multimode fiber); 10: Lens: F = 50 mm; 11: Input Camera.

4.2. Comparison of coupling efficiency

This experimental setup as shown in shaded rectangle in Fig. 3 was used for measuring the coupling efficiency of the two SuC-PCFs (D_{core} = 2 µm, D_{core} = 6.2 µm) and of the tapered-PCF.

Optics EXPRESS

A power meter was positioned after the objective lens and at the fiber output (P_{in} and P_{out} in Fig. 3) for measuring the coupling efficiency and the transmission losses. The input power was fixed at 5.15 mW. Each measurement was realized after positioning anew the fiber on the alignment system. An average of coupling efficiency was calculated across seven measurements for each fiber. The results plotted in Fig. 4, show that the tapered fiber allows a better coupling efficiency (~ 60%) than the 2 µm-PCF (~ 21%), while the 6.2 µm-PCF exhibits the highest coupling efficiency (~ 63%). It is worth noting that these measurements include both the assessment of coupling efficiency and the quantification of transmission losses. Therefore, the slight difference between the tapered-PCF and the 6.2 µm-PCF highlights the high quality of the taper fabrication process yielding very slight additional losses. In addition, the tapered fiber has a better coupling efficiency reproducibility compared to the 2 µm-PCF, with a relative standard deviation of 1% against 12%, respectively. These results validate the fabrication and the use of a tapered-PCF with an initial large core size (D_{core} = 6.2 µm) for improving the coupling efficiency and reliability to a small core (D_{core} = 1.7 µm).

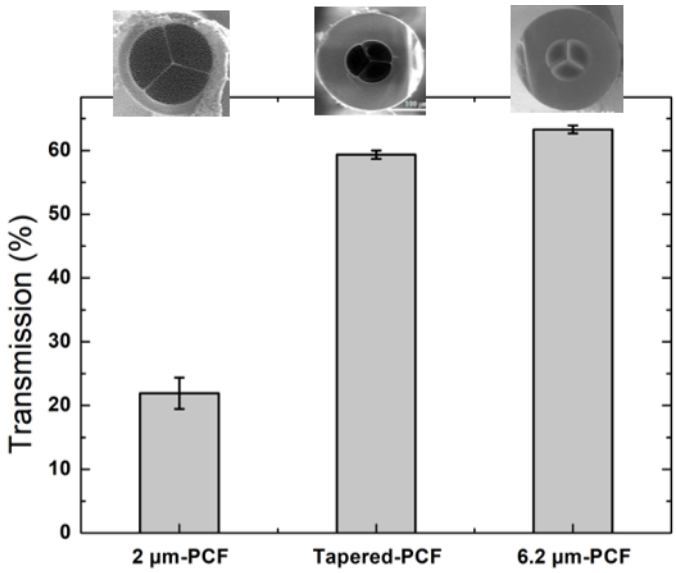

Fig. 4. Average of light transmission measurements for a SuC-PCFs (D_{core} = 2 µm and D_{core} = 6.2 µm) and a tapered-PCF; error bars represent the relative standard deviation (RSD) across seven measurements.

4.3. SERS measurements

To assess the SERS performance, signal from 4-Aminothiophenol (ATP), which is a well-known Raman active molecule and has a strong Raman cross section was used and it exhibits two very intense peaks at 1080 cm^{-1} and 1590 cm^{-1} that correspond to the stretching modes νCS, 7a and νCC, 8a, respectively. The fibers were functionalized with gold nanoparticles (AuNPs) and ATP following this protocol (Fig. 5(a)): a solution containing 2% (3-Aminopropyl) triethoxysilane (APTES) solution in acetone is infiltrated into the fibers to functionalize the silica walls. Then, the Au NPs in solution (60 nm diameter, ~10^{10} particles/mL, BBI solution) were attached to the immobilized APTES molecules by injecting them into the fibers using a customized syringe pump [21]**.** Figure 5(b) shows the anchoring of Au NPs inside the fiber. Finally, solution of ATP (1 mM) was injected into the fibers to bind to the previously immobilized AuNPs. Thereafter, the fibers were flushed with water and air to remove unbound ATP molecules and avoid the blockage

Optics EXPRESS

at the fiber tip. In addition, in order to conduct a comparative study between the signal obtained using the tapered-SuC-PCF and a conventional cuvette for a 1 mM ATP solution, we prepared ATP solution mixed with colloidal solution of 60 nm spherical Au nanoparticles, resulting in a 1 mM ATP concentration. This mixture was filled into the cuvette with a width of 1 mm.

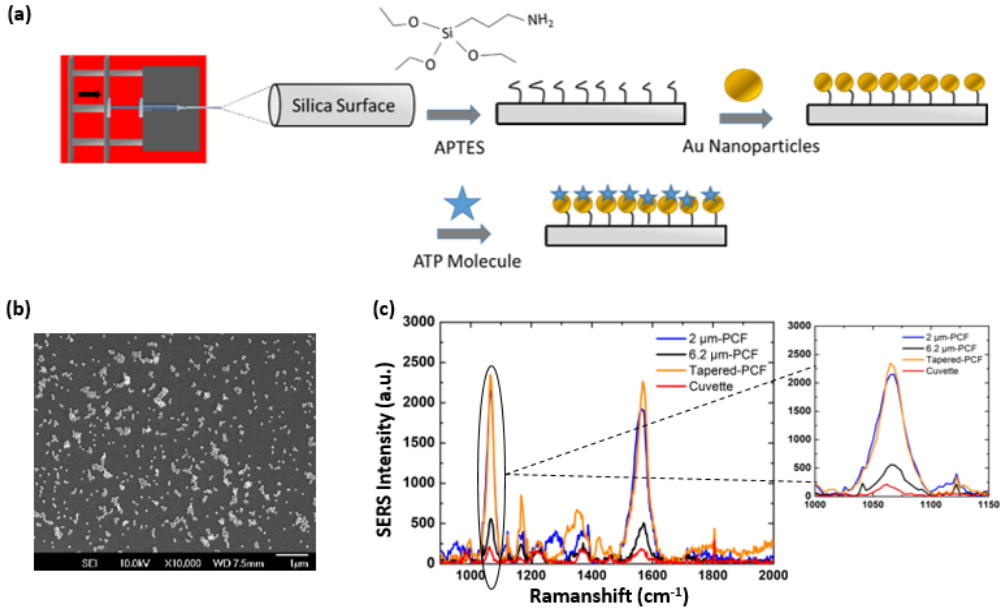

Fig. 5. (a) Schematic of the functionalization protocol inside the holes of the SuC-PCF with AuNPs and resultant binding of ATP molecules to it. (b) SEM picture of the anchored Au NPs inside the fiber. (c) SERS spectra of ATP molecules measured with cuvette-1 mm, 2 µm-PCF, 6.2 µm-PCF and the tapered-PCF and zoomed image of the spectral intensity of 1080 cm^{-1} peak.

The intensity of 1080 cm^{-1} peak was used to compare the sensitivity of both SuC-PCFs and of tapered-SuC-PCF to a cuvette. The Raman spectra of ATP molecule obtained with functionalized both SuC-PCFs and the tapered-SuC-PCF are shown in Fig. 5(b). As expected, the measured Raman signal is much weaker (~4 times) with the 6.2 µm-PCF than the 2 µm-PCF. The tapered-PCF and the 2 µm-PCF exhibit a similar sensitivity, with a slightly higher intensity (9%) of the peak measured with the tapered-PCF. Moreover, the signal acquired with the tapered-SuC-PCF was found to be twelve times higher than the signal measured with the cuvette (Fig. 5(b)). These results also underscore the superior coupling efficiency of the tapered-PCF that compensates the shorter length of the taper waist (4 cm) than the length (10 cm) of the 2 µm-PCF.

4.4. Determination of the reliability of the tapered-PCF fiber in comparison with 2 µm-PCF

In our experimental setup, the optimization of signal involved a meticulous adjustment of fiber to the focused laser beam. Specifically, we moved the fiber in front of the focused beam by monitoring the reflected beam on the fiber facet with a CCD camera. Then the fiber position is fine-tuned by optimizing signal at a specific Raman peak of interest for each measurement. We compared the reliability between the two fibers to show the improvement of the tapered fiber to 2 µm-PCF. Reliability measurements were realized by measuring the reproducibility (the ability of a single sensor to give uniform signals across various measurements) and the repeatability (the capacity of several sensors prepared under the same conditions to give uniform signals).

Optics EXPRESS

To evaluate the reproducibility of the SERS measurements several fibers were prepared and for each fiber, seven measurements were carried out, and then the relative standard deviation (RSD) was calculated for each fiber to deduce the overall reproducibility. To determine the RSD in repeatability of the SERS measurements, we prepared several fibers under exactly the same conditions. Then, for each fiber, we averaged the intensity over all measurements. Then, the RSD from these different averaged intensities was calculated to deduce the repeatability. It is worth noting that between each measurement, we removed the fiber (or the tapered fiber) and put it back into the optical system. Three Raman spectra were recorded for each set of data, and subsequently, they were averaged to ensure robust and reliable SERS assessments.

The results shown in Fig. 6(a) and (b), demonstrate that a better reproducibility of the measurements was obtained with the tapered fiber than the 2 µm-PCF, yielding a reduction of the RSD from 11.08% (2 µm-PCF) to 3.2% (tapered fiber).

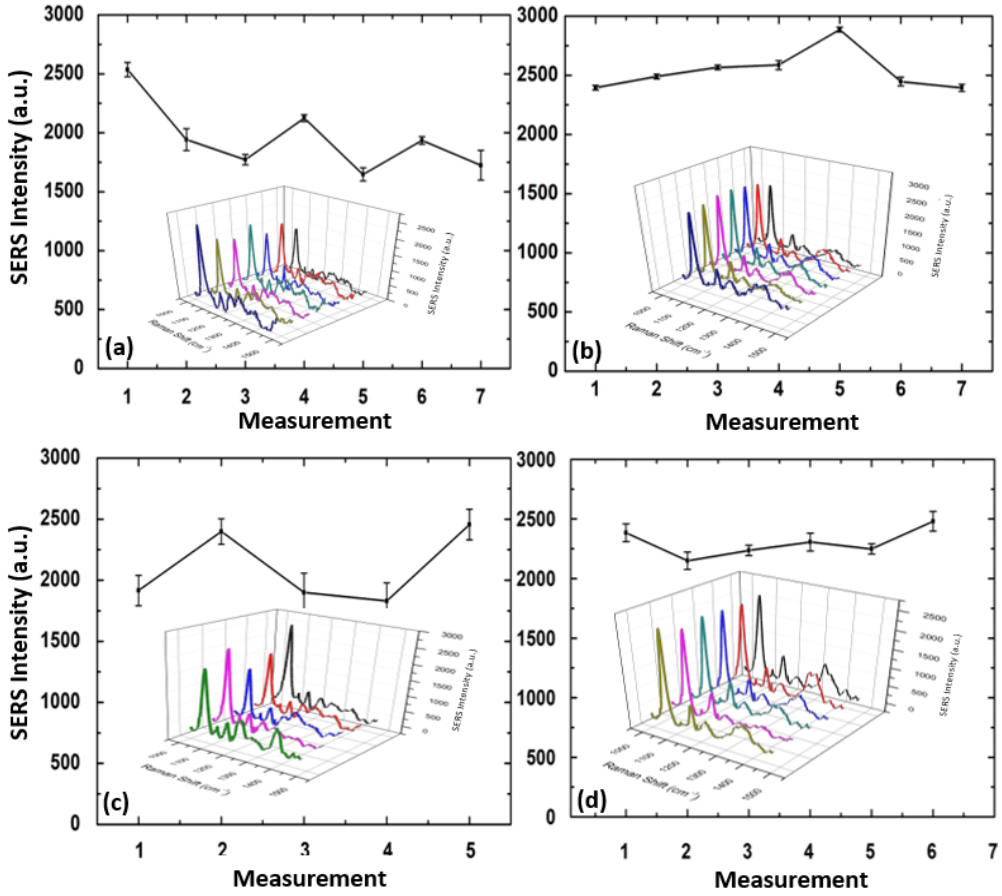

Fig. 6. Variations of the Raman intensity of the peak at 1080 cm^{-1} of ATP (seven measurements) acquired from (a) one fiber of 2 µm-PCF and (b) one tapered fiber. Error bars represents the SD of the seven measurements. Variations in the peak Raman intensity at 1080 cm^{-1} with (c) five different 2 µm-PCF fibers and (d) six different tapered fibers. Three Raman spectra were recorded for each measurement.

A better repeatability of the measurements was also obtained with the tapered fiber, with a RSD as low as 3.84% while it is 15.23% for the 2 µm-PCF ((Fig. 6(c) and (d)). It shows a significant improvement by using the tapered fiber. These results emphasize the interest of tapered-SuC-PCF

Optics EXPRESS

as practical and highly sensitive SERS sensor with minimized signal variations that may arise due to slight misalignments encountered during measurements. Such small misalignments, often inevitable in practical measurements, can lead to significant signal fluctuations with small core size fiber, but the tapered-PCF mitigates this issue, making it a reliable and robust choice for precise and consistent SERS applications.

4.5. Test of a "plug and play" type system with the tapered-PCF

In this study, we utilized a "bare fiber" connector (BFA Thorlabs, Fig. 7(a)) with an inner diameter of 850 µm to secure the un-tapered part of the 6 µm-PCF (D_{ext} = 815 µm) and test the reliability of SERS measurements by simply plugging this connector. Initially, we conducted the first measurement by connecting the taper to the fiber connector system (FC/PC fiber adapter plate) and aligning it to the laser beam. Subsequently, we carried out additional measurements without the need for realignment. The BFA connector was easily removed and reinserted to assess the reproducibility of the SERS measurements using this system.

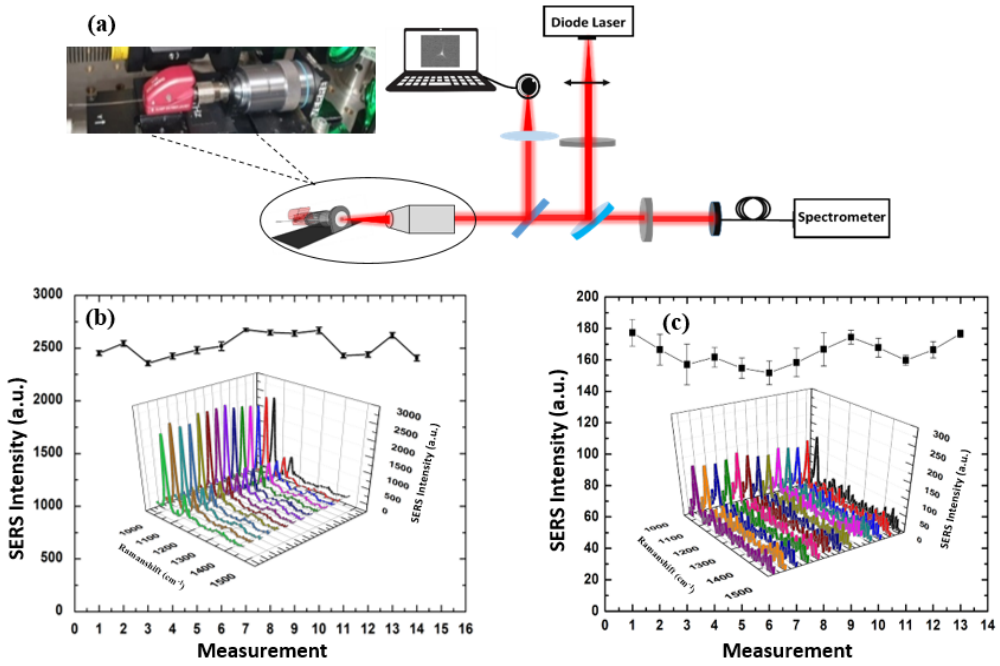

Fig. 7. (a) Experimental setup used for SERS measurements with the plug and play system. The inset image represents a photography of the plug and play system with the tapered SuC-PCF inserted within a bare fiber connector. (b) Raman intensity variations of the peak at 1080 cm^{-1} of 1 mM of ATP (fourteen measurements) and (c) 100 nM of ATP (thirteen measurements) with the PCF-tapered inserted in the system. Error bars represents the SD of the all measurements.

The results of this experiment, focusing on the ATP analyte at a concentration of 1 mM, are shown in Fig. 7(b), revealing highly reproducible SERS signals with only a negligible variation (RSD of 4.5%). In addition, further measurements were conducted with the same ATP analyte but at a lower concentration of 100 nM, which is the limit of detection (LOD) achieved by our system. The results, depicted in Fig. 7(c), indicate an RSD of 5.01%. These results demonstrate the excellent performance of this plug and play type system for SERS sensing, as it allows for reliable measurements without the necessity of realigning the fiber each time, providing a

Optics EXPRESS

user-friendly and dependable solution, even with the challenges posed by a low concentration of analyte.

In addition to its advantages in term of ease of use and cost reduction, this plug and play type system can be implemented as an optofluidic biosensor to test biomarkers in body fluids. In this environment, it is often necessary to perform accurate and repeatable measurements on a large number of patient's samples. The plug and play type system could increase the efficiency and speed of these measurements, while reducing the risk of errors related to the alignment of the fiber. However, it is important to note that this system requires further optimization and refinement to translate it as a practically relevant biosensor for medical applications.

5. Conclusion

In this study, first demonstration of fabrication and performance characterization of a SERS platform using tapered-SuC-PCF as an opto-fluidic sensor is realized and it exhibits excellent improvement in measurements. A comparison of its superior performance with a standard SuC-PCF was investigated in terms of coupling efficiency, sensitivity and reliability in measurements. Moreover, these performances allowed us to demonstrate the use of SERS fiber platforms in a "plug and play" configuration with standard Raman spectrometers and resulting in an excellent reproducibility with only ~ 5% variation in signal (at 1 mM and 100 nM of ATP). Achieved results could potentially open up the way to envisage the production of high-performance SERS probes for the analysis of body fluids and an easy to use probe for practical biosensing applications.

Funding. Agency for Science, Technology and Research; National Research Foundation Singapore; Conseil Régional Aquitaine; Centre National de la Recherche Scientifique; Agence Nationale de la Recherche.

Acknowledgments. This work is supported by institutional grants from the National Research Agency under the Investments for the future program with the reference ANR-18-EURE-0017 TACTIC, the ANR-NRF grant NRF2021-NRF-ANR002 FUNSENS, the project "FibOsome" funded by Nouvelle Aquitaine. This work was conducted within the frame of the International Research Project "FiberMed" from CNRS, A*STAR and Univ. Limoges.

Disclosures. The authors declare no conflicts of interest.

Data availability. Data underlying the results presented in this paper are not publicly available at this time but may be obtained from the authors upon reasonable request.

References

1. S.-Y. Ding, J. Yi, J.-F. Li, *et al.*, "Nanostructure-based plasmon-enhanced Raman spectroscopy for surface analysis of materials," Nat. Rev. Mater. **1**(6), 16021 (2016).
2. U. S. Dinish, G. Balasundaram, Y.-T. Chang, *et al.*, "Actively Targeted In Vivo Multiplex Detection of Intrinsic Cancer Biomarkers Using Biocompatible SERS Nanotags," Sci. Rep. **4**(1), 4075 (2014).
3. U. S. Dinish, G. Balasundaram, Y. T. Chang, *et al.*, "Sensitive multiplex detection of serological liver cancer biomarkers using SERS-active photonic crystal fiber probe: SERS active photonic crystal fiber probe for multiplex biomarker detection," J. Biophotonics **7**(11-12), 956–965 (2014).
4. K. K. Maiti, A. Samanta, M. Vendrell, *et al.*, "Multiplex cancer cell detection by SERS nanotags with cyanine and triphenylmethine Raman reporters," Chem. Commun. **47**(12), 3514–35162 (2011).
5. H. Kang, S. Jeong, Y. Park, *et al.*, "Near-Infrared SERS Nanoprobes with Plasmonic Au/Ag Hollow-Shell Assemblies for In Vivo Multiplex Detection," Adv. Funct. Mater. **23**(30), 3719–3727 (2013).
6. J. Xu, C. Li, H. Si, *et al.*, "3D SERS substrate based on Au-Ag bi-metal nanoparticles/MoS2 hybrid with pyramid structure," Opt. Express **26**(17), 21546–21557 (2018).
7. P. L. Stiles, J. A. Dieringer, N. C. Shah, *et al.*, "Surface-Enhanced Raman Spectroscopy," Annu. Rev. Anal. Chem. **1**(1), 601–626 (2008).
8. M. G. Albrecht and J. A. Creighton, "Anomalously intense Raman spectra of pyridine at a silver electrode," J. Am. Chem. Soc. **99**(15), 5215–5217 (1977).
9. D. L. Jeanmaire and R. P. V. Duyne, "Surface Raman Spectroelectrochemistry," J. Electroanal. Chem. **84**(1), 1–20 (1977).
10. M. Moskovits, "Surface-enhanced Raman spectroscopy: a brief retrospective," J. Raman Spectrosc. **36**(62-7), 485–496 (2005).
11. S. Nie, "Probing Single Molecules and Single Nanoparticles by Surface-Enhanced Raman Scattering," Science **275**(5303), 1102–1106 (1997).
12. H. Ko, S. Singamaneni, and V. V. Tsukruk, "Nanostructured Surfaces and Assemblies as SERS Media," Small **4**(10), 1576–1599 (2008).

Optics EXPRESS

13. C. Zhang, S. Z. Jiang, Y. Y. Huo, *et al.*, "SERS detection of R6 G based on a novel graphene oxide/silver nanoparticles/silicon pyramid arrays structure," Opt. Express **23**(19), 24811–24821 (2015).
14. C. Zhang, C. Li, J. Yu, *et al.*, "SERS activated platform with three-dimensional hot spots and tunable nanometer gap," Sens. Actuators, B **258**, 163–171 (2018).
15. K. C. Bantz, J. T. Rodriguez, R. S. Ring, *et al.*, "Stabilization of Silver and Gold Nanoparticles: Preservation and Improvement of Plasmonic Functionalities," Phys. Chem. Chem. Phys. **13**, 11551–115627 (2011).
16. G. J. Kovacs, R. O. Loutfy, P. S. Vincett, *et al.*, "Distance dependence of SERS enhancement factor from Langmuir-Blodgett monolayers on metal island films: evidence for the electromagnetic mechanism," Langmuir **2**(6), 689–694 (1986).
17. E. Hao and G. C. Schatz, "Electromagnetic fields around silver nanoparticles and dimers," J. Chem. Phys. **120**(1), 357–366 (2004).
18. J. P. Camden, J. A. Dieringer, J. Zhao, *et al.*, "Controlled Plasmonic Nanostructures for SurfaceEnhanced Spectroscopy and Sensing," Acc. Chem. Res. **41**(12), 1653–1661 (2008).
19. U. S. Dinish, F. Beffara, G. Humbert, *et al.*, "Surface-enhanced Raman scattering-active photonic crystal fiber probe: Towards next generation liquid biopsy sensor with ultra-high sensitivity," J. Biophotonics **12**(11), e201900027 (2019).
20. Y. Han, S. Tan, M. K. K. Oo, *et al.*, "Towards Full-Length Accumulative Surface-Enhanced Raman Scattering-Active Photonic Crystal Fibers," Adv. Mater. **22**(24), 2647–2651 (2010).
21. F. Beffara, J. Perumal, A. Puteri Mahyuddin, *et al.*, "Development of highly reliable SERS-active photonic crystal fiber probe and its application in the detection of ovarian cancer biomarker in cyst fluid," J. Biophotonics **13**(3), e201960120 (2020).
22. A. Khetani, V. S. Tiwari, A. Momenpour, *et al.*, "Monitoring of adenosine within hollow core photonic crystal fiber by surface enhanced Raman scattering (SERS)," in *2011 11th IEEE International Conference on Nanotechnology* (2011), 973–977.
23. Y. Zhang, C. Shi, C. Gu, *et al.*, "Liquid core photonic crystal fiber sensor based on surface enhanced Raman scattering," Appl. Phys. Lett. **90**(19), 193504 (2007).
24. Y. Guo, M. K. Khaing Oo, K. Reddy, *et al.*, "Ultrasensitive Optofluidic Surface-Enhanced Raman Scattering Detection with Flow-through Multihole Capillaries," ACS Nano **6**(1), 381–388 (2012).
25. N. Zhang, G. Humbert, T. Gong, *et al.*, "Side-channel photonic crystal fiber for surface enhanced Raman scattering sensing," Sens. Actuators, B **223**, 195–201 (2016).
26. F. Beffara, G. Humbert, J.-L. Auguste, *et al.*, "Optimization and performance analysis of SERS-active suspended core photonic crystal fibers," Opt. Express **28**(16), 23609–23619 (2020).
27. M. K. Khaing Oo, Y. Han, J. Kanka, *et al.*, "Structure fits the purpose: photonic crystal fibers for evanescent-field surface-enhanced Raman spectroscopy," Opt. Lett. **35**(4), 466–468 (2010).
28. N. S. Kapany and J. J. Burke, "Waveguide Mode Lauching," in *Optical Waveguides, Quantum Electronics–Principles and Applications* (Academic Press, 1972), 159–179.
29. M. Skorobogatiy and J. Yang, *Fundamentals of Photonic Crystal Guiding* (Cambridge University, 2009).
30. T. G. Euser, J. S. Y. Chen, M. Scharrer, *et al.*, "Quantitative broadband chemical sensing in air-suspended solid-core fibers," J. Appl. Phys. **103**(10), 103108 (2008).